Arabian Journal of Chemistry (2020) **13**, 6403–6411

King Saud University

Arabian Journal of Chemistry

www.ksu.edu.sa
www.sciencedirect.com

ORIGINAL ARTICLE

Preparation of benzo[4,5]thiazolo[3,2-a]chromeno [4,3-d]pyrimidin-6-one derivatives using $MgO\text{-}MgAl_2O_4$ composite nano-powder

Mehdi Khalaj *

Department of Chemistry, Buinzahra Branch, Islamic Azad University, Buinzahra, Iran

Received 2 April 2020; accepted 30 May 2020
Available online 12 June 2020

KEYWORDS

$MgO\text{-}MgAl_2O_4$;
Nanocomposite;
Benzo[4,5]thiazolo[3,2-a]chromeno[4,3-d]pyrimidin-6-ones;
Pyrimidines;
HSBM technique

Abstract $MgO\text{-}MgAl_2O_4$ nanocomposite was prepared from the co-precipitation of $Mg(NO_3)_2$ and $Al(NO_3)_3$ salts, characterized by X-ray diffraction (XRD), transmission electron microscopy (TEM), energy-dispersive X-ray spectroscopy (EDS) and fourier transform infrared spectroscopy (FTIR) techniques and evaluated in the synthesis of thirty five derivatives of benzo[4,5]thiazolo[3,2-a]chromeno[4,3-d]pyrimidin-6-ones (**d_1-d_{34}**) *via* the multi-component reaction of 4-hydroxycoumarins, aldehydes, and 2-aminobenzothiazole derivatives under solvent free condition. The catalytic activity of $MgO\text{-}MgAl_2O_4$ nanocomposite and the synthesis of the above mentioned compounds were investigated under thermal solvent free (times: 1.4–3 h; yields: 75–95%), ultrasonic irradiation (US) conditions (times: 1–2.5 h; yields: 69–97%) and using high-speed ball milling (HSBM) technique (times: 0.7–2.5 h; yields: 67–97%). In all cases, the products were obtained in excellent yields. Nuclear Magnetic Resonance (NMR) and MASS spectroscopy were used to characterize the structure of the desired product. The mechanism for the preparation of compounds **d_1-d_{34}** was proposed and confirmed by ^{1}H NMR investigations.

1. Introduction

The pyrimidine rings combined with thiazol, chromene and pyran heterocycles, known as important privileged heterocyclic scaffolds, are found in a variety of drugs and natural products. In particular, fused thiazolo and chromenopyrimidines have attracted much attention in medical chemistry due to their significant therapeutic and biological activities. Fused thiazolo and chromenopyrimidines have shown significant activity against a number of pathogens and diseases such as anti-inflammatory, antiparkinsonian, anti-HIV, anti-HSV-1 and cardiovascular agents (Selvam et al., 2012; Amr et al., 2008; Mohamed et al., 2010; Cumming at al., 2004). The antioxidant and antimicrobial activities of some thiazolopyrimidines have been reported by Youssef and Amin (2012). Some fused thiazolo[3,2-a] pyrimidine derivatives have shown significant antibacterial activity against diverse pathogenic strains such

* Corresponding author.
E-mail address: Khalaj_mehdi@yahoo.com.
Peer review under responsibility of King Saud University.

Production and hosting by Elsevier

https://doi.org/10.1016/j.arabjc.2020.05.041
1878-5352

as Staphylococcus aureus ATCC 6538 and Pseudomonas aeruginosa ATCC 9027 (bacteria) (Afradi et al., 2017).

A Literature view reveals that fused thiazolo and chromenopyrimidines have been synthesized using different procedures e.g. a multi-step reaction of 2-hydroxybenzaldehyde, malononitril, DMF-acetal and amines (Rai et al., 2010), treatment of benzochromenes with acetic anhydride under reflux conditions (Abozeid et al., 2019), and a three-component condensation of 3,4-dihydropyrimidine-2(1H)-thiones, aldehydes and chloroacetyl chloride catalyzed by Fe_3O_4@L-arginine nanoparticles (Afradi et al., 2017). Moreover, the catalytic preparation of a library of thiazolopyrimidines has been performed under thermal and microwave conditions in the presence of different catalysts such as SiO_2–$ZnBr_2$ (Devineni1 et al., 2019), Low melting glycerol/proline mixture (Mohire et al., 2019), ionic liquids (Arya et al., 2018; Khandelwal et al., 2015), and *para*-toluene sulfonic acid (Roudbaraki et al., 2019).

On the other hands, fused pyrimidines containing both thiazol and chromene moieties were prepared *via* cyclization of isatin, cyclohexane-1,3-diones, and 2-hydroxy-4H-benzo[4,5]thiazolo[3,2-a]pyrimidin-4-ones by Jannati and Esmaeili (2018). Recently, a series of benzo[4,5]thiazolo[3,2-a]chromeno[4,3-d]pyrimidin-6-ones were prepared by a the three-component condensation of 4-hydroxycoumarins, 2-aminobenzothiazoles, and aldehydes using an ionic liquid (Sagar Reddy and Jeong, 2016), sodium lauryl sulfate (SLS) micelles (Sahu, 2016a), and hydrotalcite (Sahu, 2016b) as efficient catalysts. This procedure is simple and can be extended to different substrates.

Although the synthesis of fused pyrimidines has been widely investigated, the development of synthetic methodologies for the synthesis of fused pyrimidines is in demand due to their wide applications as pharmacophores.

On the other hands, heterogeneous catalysis by nanomaterials has a major key role in chemical transformations as they provide approaches for environmental protection. Nanocomposite materials are an important class of heterogeneous catalysts, which has been used widely in organic synthesis and other chemical transformations and have provided reasonable good results in term of reaction parameters such as time and yield (Sharma et al., 2015; Zhan et al., 2020; Wang et al., 2019; Zhang et al., 2020; Feng et al., 2020). Therefore, new research is needed to find high-performance catalytic systems to increase productivity.

Recently, many researchers have considered the use of metal-based nanocomposites due to their high specific surface area and proper catalytic activity. Many synthetic organic reactions have promoted by metal oxides nanocomposites and they can contributed significantly to the design of novel heterocycles. Metal oxides have crystalline structures that enhance the catalytic properties of these compounds. Moreover, the combination of metal oxides, especially on a nanoscale, makes it possible to modify and improve the specific surface area of materials, increase active sites, and thus increase the catalytic capacity of these compounds. Therefore, trying to synthesize metal nanocomposites is an interesting topic in the field of nanocatalysts (Bhaskaruni et al., 2020; Shafighi et al., 2018; Harikrishna et al., 2020; Hillary et al., 2017; Fang et al., 2020; Wang et al., 2020; Asgari et al., 2020). Therefore, in continue of our investigations on the preparation of heterocyclic compounds (Khalaj et al., 2019, 2018a, 2018b; Varmazyar et al., 2019a, 2019b), in this work, we aim at synthesizing a variety of benzo[4,5]thiazolo[3,2-a]chromeno[4,3-d]pyrimidin-6-one derivatives using MgO-$MgAl_2O_4$ composite nano powder from the three-component reaction of 4-hydroxycoumarin, aryl aldehydes, and 2-aminobenzothiazole derivatives (Scheme 1).

2. Experimental

2.1. Preparation of MgO-$MgAl_2O_4$ nanocomposite

To a solution of $Mg(NO_3)_2$ (20 mmol) and $Al(NO_3)_3$ (20 mmol) in 200 mL of water, 100 mL of ammonia solution (15%) were added dropwise under vigorous magnetic stirring until the pH increased to 12. The resulting precipitate was dried at 80 °C after separation and washing with water. MgO-$MgAl_2O_4$ was obtained after calcination at 800 °C for 3 h.

2.2. General procedure

Method A: A mixture of 4-hydroxycoumarin (**a**, 1 mmol), benzaldehyde (**b**, 1 mmol), 2-aminobenzothiazole (**c**, 1 mmol), and MgO-$MgAl_2O_4$ (0.05 g) was heated on an oil bath at 100 °C. The Hot ethanol was used for catalyst seperation from the organic phase after the reaction was complete, as monitored by TLC (eluent being *n*-hexane/ethyl acetate: 4/1). At last, the pure product was obtained via recystallization from EtOH.

Method B: The oil bath was replaced by an ultrasonic bath. All parameters were the same as those in method A, except for the ultrasonic irradiation at 80 °C.

Method C: Similar to method A, the starting materials were mixed and milled in a 10 mL volume stainless steel grinding vial using stainless steel balls (diameter: 6 mm; mass: 1.04 g)

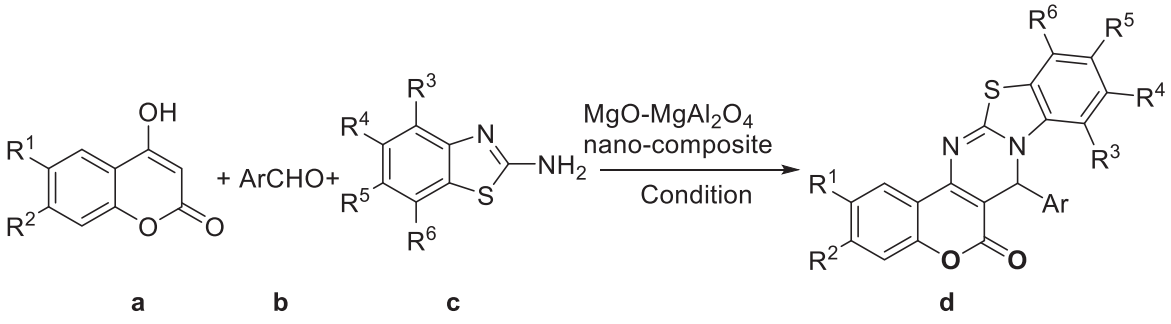

Scheme 1 Preparation of benzo[4,5]thiazolo[3,2-a]chromeno[4,3-d]pyrimidin-6-one derivatives using MgO-$MgAl_2O_4$ nanocomposite.

at 25 Hz and 70 °C. The next steps were similar to those in method A.

3. Results and discussion

3.1. Catalyst characterization

Fig. 1 shows the TG and DTG analyses of crude precursors of MgO-$MgAl_2O_4$ nanocomposite. The weight of the sample decreased with increasing temperature. About 44% of mass loss occurred in the temperature range of 100–350 °C due to the evaporation of physisorbed water and the transformation of $Mg(OH)_2$ to MgO and $Al(OH)_3$ to Al_2O_3 oxides (Ewais et al., 2017). DTA analysis shows two exothermic peaks below 400 °C, indicating the precursor decomposition. The endothermic peak above 650 °C is due to the conversion of MgO and Al_2O_3 to $MgAl_2O_4$ spinel (Zhang et al., 2004). Thus, 800 °C was selected as the calcination temperature of the crude precursor to assure the formation of MgO-$MgAl_2O_4$ nanocomposite.

The X-ray diffraction (XRD) pattern of MgO-$MgAl_2O_4$ nanocomposite is shown in Fig. 2. The XRD pattern consists of pronounced peaks centered at 36.9, 42.8, 62.2, 74.6, and 78.5 [2θ°], corresponding to the cubic phase of MgO (JCPDS: 01–087-0651) and those located at 31.3, 36.9, 44.9, 49.1, 55.7, 59.4, 65.3, 77.4, and 82.7 [2θ°] are related to the cubic phase of $MgAl_2O_4$ spinel structure (JCPDS: 01-073-0559). No impurity peaks were detected (Rahmani Vahid and Haghighi, 2016).

The surface morphology of MgO-$MgAl_2O_4$ nanocomposite was investigated by TEM analysis (Fig. 3) and the results show that the nanocomposite consists of small spherically shaped particles with a little agglomeration. The average size is less than 100 nm. The EDS analysis of MgO-$MgAl_2O_4$ nanocomposite confirms that the molar ratio of Mg:Al:O is about 1:1:2.

The FT-IR spectrum of MgO-$MgAl_2O_4$ nanocomposite shows a broad band at about 3200–3500 cm^{-1}, which is due to the H-O stretching vibration from the absorbed water. The two peaks present below 700 cm^{-1} correspond to the vibrations of Al-O-Mg, Mg-O, and Al-O bonds (Ewais et al., 2017; Tripathy and Bhattacharya, 2013), indicating the formation of MgO and $MgAl_2O_4$ spinel (Fig. 4).

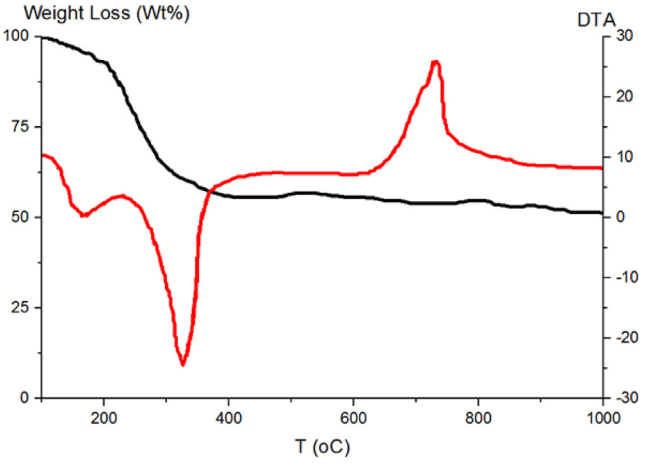

Fig. 1 TGA and DTA analysis of crude materials.

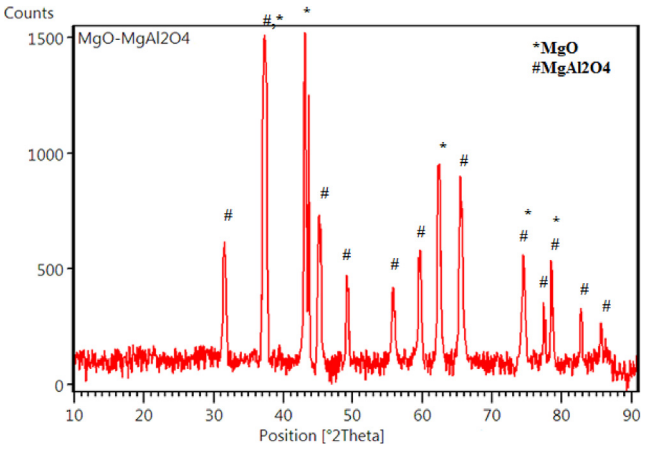

Fig. 2 XRD pattern of MgO-$MgAl_2O_4$ nanocomposite.

3.2. Catalytic evaluation

At first, the three-component reaction of 4-hydroxycoumarin, benzaldehyde, and 2-aminobenzothiazole was selected for investigation under different conditions. The reactions were carried out using different solvents, temperatures and catalyst dosages and 0.05 g of MgO-$MgAl_2O_4$ nanocomposite (Table 1). As observed in Table 1, acceptable product yields were not obtained using any of the solvents screened, while excellent product yields were achieved under solvent free conditions at lower reaction times. Next, the same model reaction was investigated for the effect of different temperatures in the 25–120 °C range on the product formation. According to the results, no products form when the temperature is below 80 °C. Clearly, the productivity of the reaction significantly increased by raising the temperature from 80 to 100 °C within short reaction times. However, higher temperatures do not improve the rate and efficiency of the reaction. Afterwards, the effect of catalyst dosages on the reaction process was investigated. As shown in Table 1, the reaction proceeds faster by increasing the catalyst dosage up to 0.05 g, while there are no significant changes in the reaction progress using higher catalyst dosages.

Finally, 0.05 g of the catalyst, temperature of 100 °C and solvent free conditions were determined as optimized reaction conditions. In comparison with some other catalysts including MgO, Al_2O_3 and $MgAl_2O_4$, MgO-$MgAl_2O_4$ nanocomposite shows better results in terms of reaction parameters such as time and product yield (Table 1).

Consequently, under the optimal conditions, the generality of this method was studied in the transformation of a series of substituted aldehydes into the corresponding 7-aryl-6H,7H-benzo[4,5]thiazolo[3,2-a]chromeno[4,3-d]pyrimidin-6-ones in good to excellent yields (Table 2). As shown in Table 2, the reaction of 2-aminobenzothiazoles, different aldehydes, and 4-hydroxycoumarins proceeded efficiently to form products in high yields mostly.

Generally, aromatic aldehydes containing electron donating groups have shown to be more reactive than those with electron withdrawing groups. In addition, *ortho*-substituted aldehydes react slowly compared to the *para* isomers. These results indicate that the electronic nature of the substituents

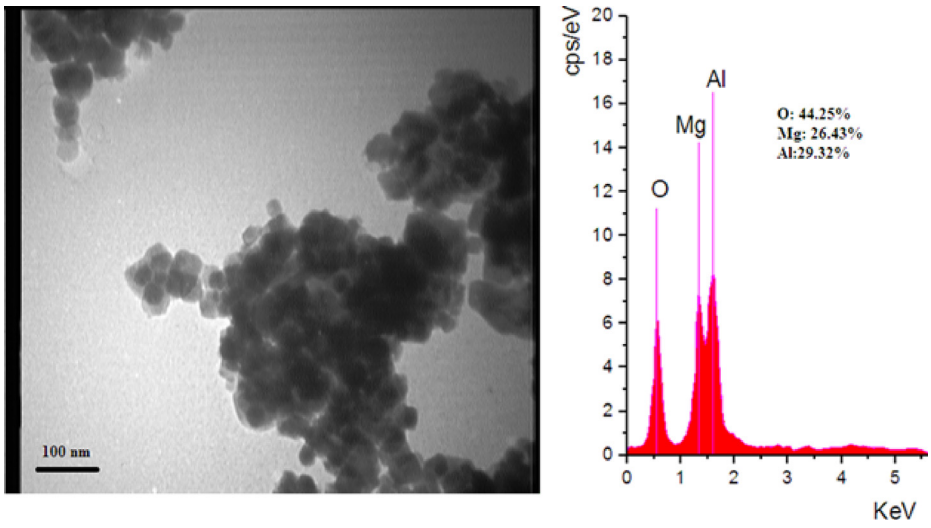

Fig. 3 TEM photograph and EDS analysis of MgO-$MgAl_2O_4$ nanocomposite.

considerably affects the reaction rates (Table 2, Entries 1–17). Heterocyclic aldehydes such as thiophene-2-carbaldehyde could also achieve good results in a short time (Table 3, Entries 4,5). Cyclohexane carbaldehyde, an aliphatic aldehyde, gave high yields in this reaction (Table 2, Entry 12).

Next, the reactions were undertaken using some substituted 4-hydroxycoumarin (6,7-dichloro-4-hydroxy-2H-chromen-2-one; 4-hydroxy-6,7-dimethoxy-2H-chromen-2-one), and 2-aminobenzothiazoles (6-methylbenzo[d]thiazol-2-amine; 6-nitrobenzo[d]thiazol-2-amine; 7-chloro-4-methylbenzo[d]thiazol-2-amine) and the results are summarized in Table 3 (Table 3, Entries 1–19). As observed, all compounds were successfully employed in the reaction and the products were formed in high yields.

The role of MgO-$MgAl_2O_4$ on the catalytic preparation of 7-aryl-6H,7H-benzo[4,5]thiazolo[3,2-a]chromeno[4,3-d]pyrimidin-6-one derivatives can be explained by drawing a plausible mechanism. Scheme 2 shows the proposed mechanism for the synthesis of compounds **d_1-d_{34}**. The reaction begins with an acid-base reaction of the aluminate anion (from $MgAl_2O_4$) and the acidic proton of the hydroxyl group of coumarin. Simultaneously the carbonyl group of aldehyde can be activated by magnesium oxide. Next, intermediate A is formed by an attack of the negative carbon of coumarin to the carbonyl group following by the removal of water. According to Reddy and Jeong (2016), the next step is the aza-Michael

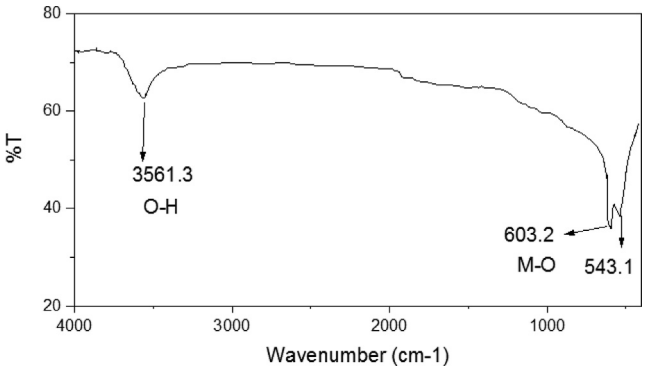

Fig. 4 FT-IR spectra of MgO-$MgAl_2O_4$ nanocomposite.

Table 1 Optimization of the reaction condition.

Entry	Catalyst (0.05 g)	Condition	Time (h)/ Yield (%)*
1	MgO-$MgAl_2O_4$ nanocomposite	EtOH, Reflux	3/25
2	MgO-$MgAl_2O_4$ nanocomposite	Et_2O, Reflux	3/-
3	MgO-$MgAl_2O_4$ nanocomposite	CH_3CN, Reflux	3/15
4	MgO-$MgAl_2O_4$ nanocomposite	Toluene, Reflux	3/30
5	MgO-$MgAl_2O_4$ nanocomposite	H_2O, Reflux	3/-
6	MgO-$MgAl_2O_4$ nanocomposite	Hexane, Reflux	3/-
7	MgO-$MgAl_2O_4$ nanocomposite	EtOAc, Reflux	3/-
8	MgO-$MgAl_2O_4$ nanocomposite	solvent-free, 100 °C	1.5/75
9	MgO-$MgAl_2O_4$ nanocomposite	solvent-free, 25 °C	3/-
10	MgO-$MgAl_2O_4$ nanocomposite	solvent-free, 80 °C	3/45
11	MgO-$MgAl_2O_4$ nanocomposite	solvent-free, 120 °C	1.4/70
12	MgO	solvent-free, 100 °C	2/60
13	$MgAl_2O_4$	solvent-free, 100 °C	3/63
14	Al_2O_3	solvent-free, 100 °C	3/-
15	MgO-$MgAl_2O_4$ nanocomposite (0.01 g)	solvent-free, 100 °C	3/35
16	MgO-$MgAl_2O_4$ nanocomposite (0.025 g)	solvent-free, 100 °C	2/65
17	MgO-$MgAl_2O_4$ nanocomposite (0.1 g)	solvent-free, 100 °C	1.5/70

* Isolated Yield; based on the preparation of 7-phenyl-6H,7H-benzo[4,5]thiazolo[3,2-a]chromeno[4,3-d]pyrimidin-6-one.

Table 2 Preparation of benzo[4,5]thiazolo[3,2-a]chromeno[4,3-d]pyrimidin-6-one derivatives using $MgO\text{-}MgAl_2O_4$ nanocomposite (Scheme 1).

Entry	**a:** R^1/R^2	**b:** Ar-CHO	**c:** $R^3/R^4/R^5/R^6$	**d**	Method A	Method B	Method C
					Time (h)/Yield (%)	Time (h)/Yield (%)	Time (h)/Yield (%)
1	H/H	PhCHO	H/H/H/H	$\mathbf{d_1}$	1.5/75	1.3/85	1/82
2	H/H	4-MePhCHO	H/H/H/H	$\mathbf{d_2}$	1.4/77	1.2/83	0.8/88
3	H/H	4-MeOPhCHO	H/H/H/H	$\mathbf{d_3}$	1.2/80	1/90	0.7/85
4	H/H	3,4,5-triMeOPhCHO	H/H/H/H	$\mathbf{d_4}$	1.2/91	1/93	0.75/90
5	H/H	2-MePhCHO	H/H/H/H	$\mathbf{d_5}$	1.6/79	1.5/83	1.3/77
6	H/H	2-MeOPhCHO	H/H/H/H	$\mathbf{d_6}$	1.6/80	1.5/83	1.3/85
7	H/H	3-MeOPhCHO	H/H/H/H	$\mathbf{d_7}$	1.4/87	1.2/86	1/90
8	H/H	4-HOPhCHO	H/H/H/H	$\mathbf{d_8}$	1.5/70	1.4/73	1/74
9	H/H	4-ClPhCHO	H/H/H/H	$\mathbf{d_9}$	2/90	1.5/95	1.2/88
10	H/H	3-ClPhCHO	H/H/H/H	$\mathbf{d_{10}}$	2/78	1.5/96	1.2/90
11	H/H	2-ClPhCHO	H/H/H/H	$\mathbf{d_{11}}$	2.5/77	2/86	1.5/83
12	H/H	$C_6H_{11}CHO$	H/H/H/H	$\mathbf{d_{12}}$	2/86	1.5/88	1.5/85
13	H/H	2-BrPhCHO	H/H/H/H	$\mathbf{d_{13}}$	2.5/93	2/90	2/91
14	H/H	3-BrPhCHO	H/H/H/H	$\mathbf{d_{14}}$	2.5/93	1.5/96	1.5/93
15	H/H	4-BrPhCHO	H/H/H/H	$\mathbf{d_{15}}$	2.5/90	1.5/96	1.4/93
16	H/H	4-NO_2PhCHO	H/H/H/H	$\mathbf{d_{16}}$	3/88	2.5/86	2/82
17	H/H	3-NO_2PhCHO	H/H/H/H	$\mathbf{d_{17}}$	3/80	2.5/83	2/84

Method A: solvent-free, 100 °C; Method B: ultrasonic irradiation, solvent-free, 80 °C; Method C: HSBM technique, solvent-free, 70 °C.

Table 3 Preparation of benzo[4,5]thiazolo[3,2-a]chromeno[4,3-d]pyrimidin-6-one derivatives using $MgO\text{-}MgAl_2O_4$ nanocomposite (Scheme 1).

Entry	**a:** R^1/R^2	**b:** Ar-CHO	**c:** $R^3/R^4/R^5/R^6$	**d**	Method A	Method B	Method C
					Time (h)/Yield (%)	Time (h)/Yield (%)	Time (h)/Yield (%)
1	H/H	4-Me_2NPhCHO	H/H/CH_3/H	$\mathbf{d_{19}}$	2/85	1.2/90	1/96
2	H/H	4-ClPhCHO	H/H/CH_3/H	$\mathbf{d_{18}}$	2/87	1.2/89	1/88
3	H/H	PhCHO	H/H/NO_2/H	$\mathbf{d_{20}}$	3/77	2.5/73	2/70
4	H/H	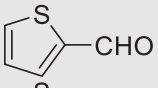	CH_3/H/H/Cl	$\mathbf{d_{21}}$	2/68	1.5/71	1/67
5	H/H	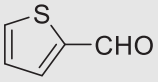	CH_3/H/Cl/H	$\mathbf{d_{22}}$	2.5/65	2/74	1.5/73
6	H/H	4-MeOPhCHO	CH_3/H/Br/H	$\mathbf{d_{23}}$	1.5/87	1.2/90	1/93
7	H/H	4-ClPhCHO	CH_3/H/Br/H	$\mathbf{d_{24}}$	2/88	1.5/89	1.3/93
8	Cl/Cl	PhCHO	H/H/NO_2/H	$\mathbf{d_{25}}$	1.5/71	1.2/69	1/78
9	Cl/Cl	4-MePhCHO	H/H/NO_2/H	$\mathbf{d_{26}}$	1.5/87	1/89	1/93
10	Cl/Cl	4-MeOPhCHO	H/H/NO_2/H	$\mathbf{d_{27}}$	1.5/95	1/90	1/97
11	Cl/Cl	3,4-diMeOPhCHO	H/H/NO_2/H	$\mathbf{d_{28}}$	1.4/88	1/96	0.9/89
12	Cl/Cl	4,5-diMeOPhCHO	H/H/NO_2/H	$\mathbf{d_{29}}$	1.5/82	1/97	1/95
13	Cl/Cl	3,4,5-triMeOPhCHO	H/H/NO_2/H	$\mathbf{d_{30}}$	1.5/85	1/87	1/84
14	Cl/Cl	3,4-diClPhCHO	H/H/NO_2/H	$\mathbf{d_{31}}$	3/82	2.5/85	2.5/87
15	Cl/Cl	4-NO_2PhCHO	H/H/NO_2/H	$\mathbf{d_{32}}$	3/85	2.5/86	2.5/87
16	Cl/Cl	4-BrPhCHO	H/H/NO_2/H	$\mathbf{d_{33}}$	3/80	2.5/89	2.5/83
17	MeO/MeO	PhCHO	H/H/NO_2/H	$\mathbf{d_{34}}$	1.5/89	1/95	1/93
18	MeO/MeO	Butyraldehyde	H/H/NO_2/H	$\mathbf{d_{35}}$	2/-	2/-	2/-
19	MeO/MeO	Hexanal	H/H/NO_2/H	$\mathbf{d_{36}}$	2/-	2/-	2/-

Method A: solvent-free, 100°C; Method B: ultrasonic irradiation, solvent-free, 80°C; Method C: HSBM technique, solvent-free, 70°C.

addition to form intermediate B, which undergoes the cyclization and dehydration to afford the desired product (Scheme 2). Another route that can be suggested is comprised from the condensation of 2-aminobenzothiazol with aldehyde (Intermediate X). Consequently, intermediate X will be convert to intermediate A *via* coumarin anion attack.

The formation of intermediates X and A was confirmed by the H-NMR investigation. Fig. 5 shows the H-NMR of reaction mixture (6,7-dichloro-4-hydroxy-2H-chromen-2-one, benzaldehyde, and 6-nitrobenzo[d]thiazol-2-amine) at the beginning of the reaction, after 30, 45, and 60 min for the preparation of product ($\mathbf{d_{25}}$). As revealed, after 30 min ben-

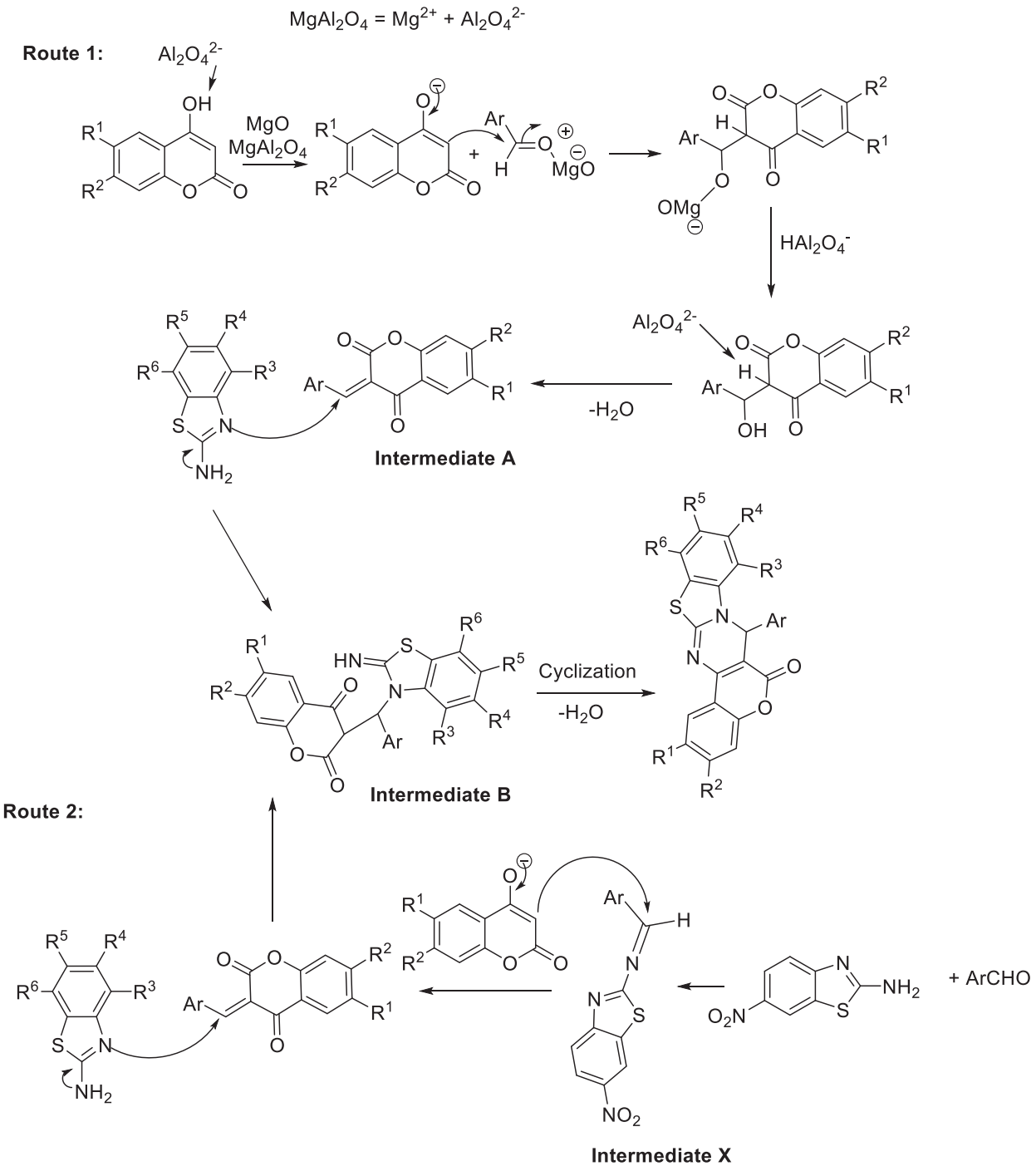

Scheme 2 Proposed mechanism.

zaldehyde is completely consumed and the intermediates A and X are formed. A few of 6,7-dichloro-4-hydroxy-2H-chromen-2-one is still remain in the reaction mixture after 30 min. The intermediate A is showed a singlet peak related to the hydrogen of alkene double bond in chemical shift 5.13 ppm, while intermediate X has an imine bond (CH = N-) which appeared as a singlet at δ = 8.78 ppm. After 45 min, intermediate B was appeared and the peaks of final products are recorded after 60 min. In comparison, in purified product none of these peaks are shown (Figure S7, Supplementary data).

Furthermore, the catalytic activity of MgO-$MgAl_2O_4$ nanocomposite and the synthesis of 7-aryl-6H,7H-benzo[4,5]thiazolo[3,2-a]chromeno[4,3-d]pyrimidin-6-one derivatives were studied under solvent free and ultrasonic irradiation (US) conditions as well as using HSBM technique. The products in both methods were obtained in excellent yields. Generally, the reaction times are decreased in US and HSBM techniques (Tables 2, 3). When aliphatic aldehydes were used, the progress of the reaction was unsuccessful and did not found to be productive in any of the worked methods (Table 3, Entries 18, 19).

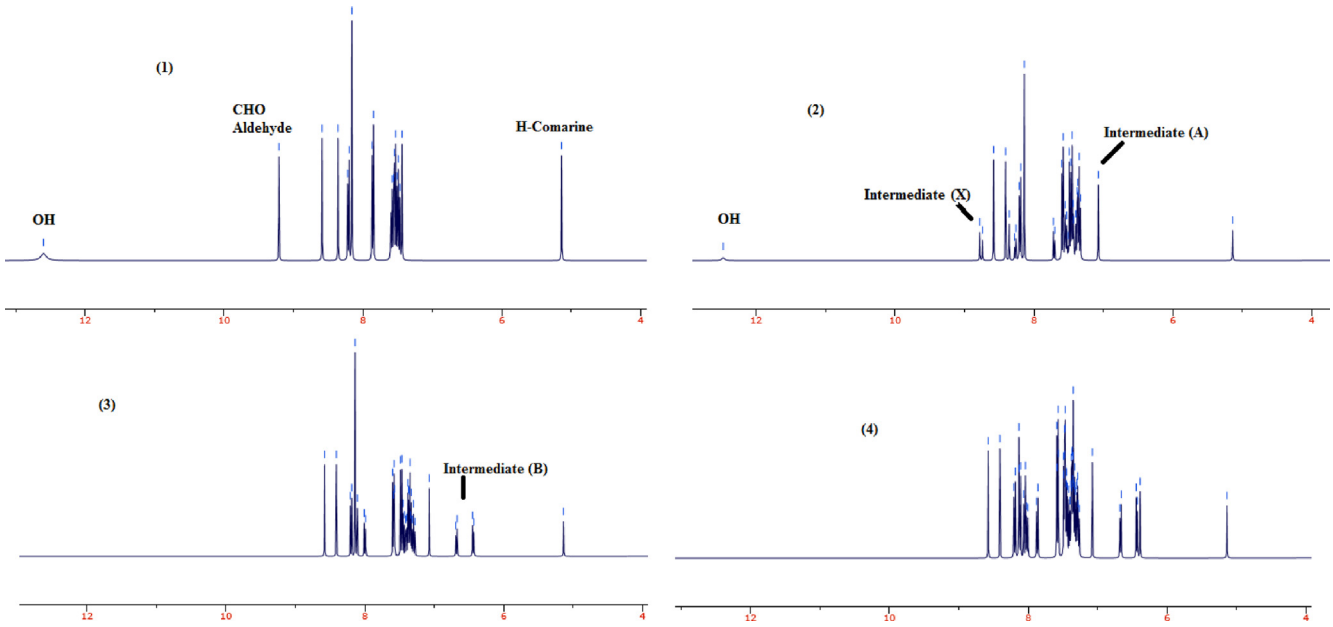

Fig. 5 ^{1}H NMR of reaction mixture at the beginning of the reaction (1), after 30 min (2) 45 (3), and 60 min (4) for the preparation of product (**d_{25}**).

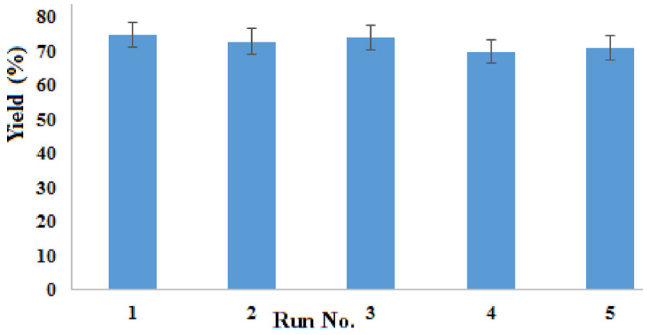

Fig. 6 reusability of MgO-$MgAl_2O_4$ nanocomposite.

Finally, in the recycling procedure, the preparation of d_1 was chosen as the model of the reaction. After completion of the reaction, the organic matter is dissolved in hot ethanol and subsequently, the catalyst was recovered by simple filtration, washed with ethanol, and dried at 100 °C to be re-used in the next cycles. MgO-$MgAl_2O_4$ nanocomposite was reused sequentially for five times without significant loss of catalytic activity (Fig. 6).

4. Conclusion

In summary, the co-precipitation synthesis and characterization of MgO-$MgAl_2O_4$ nanocomposite was reported. The sample has two cubic phase of MgO and $MgAl_2O_4$ and small spherically shaped particles without impurity. The nanocomposite is found to act as an efficient catalyst for the synthesis of some benzo[4,5]thiazolo[3,2-a]chromeno[4,3-d]pyrimidin-6-one derivatives (**d_1-d_{34}**) in excellent yields. The effect of solvent, temperature and catalyst dosage on the productivity of the reaction were investigated. The catalyst is more productive under solvent-free condition and has better results compared to MgO, Al_2O_3 and an spinel structure of $MgAl_2O_4$. In addition the nano-composite was found to have acceptable catalytic activity towards the synthesis of **d_1-d_{34}** under ultrasonic irradiation conditions and using HSBM technique. The simplicity of the preparation of ultra-fine catalyst particles as well as heterocycles is the main advantage of this procedure. Moreover, the methods described here suffer the advantages of high catalytic activity, easy catalyst separation and recycling. In addition, it can be used for a wide range of derivatives.

Declaration of interest

The authors declare that they have no declaration of interest to influence the work reported in this paper.

Acknowledgments

The laboratory support by the Islamic Azad University, Buinzahra Branch is highly acknowledged.

Appendix A. Supplementary data

Supplementary data to this article can be found online at https://doi.org/10.1016/j.arabjc.2020.05.041.

References

Abozeid, M.A., El-Kholany, M.R., Abouzeid, L.A.H., Abdel-Rahman, A.-R., El-Desoky, E.-S.I., 2019. Synthesis and Computational Analysis of New Antioxidant and Antimicrobial Angular Chromenopyrimidines. J. Heterocyclic Chem. 56, 2922–2933.

Afradi, M., Foroughifar, N., Pasdar, H., Moghanian, H., Foroughifar, N., 2017. Facile green one-pot synthesis of novel thiazolo[3,2-a] pyrimidine derivatives using Fe_3O_4@L-arginine and their biolog-

ical investigation as potent antimicrobial agents. Appl. Organometal. Chem. 31, e3683.
Amr, A.-E.-G., Maigali, S.S., Abdulla, M.M., 2008. Synthesis, and analgesic and antiparkinsonian activities of thiopyrimidine, pyrane, pyrazoline, and thiazolopyrimidine derivatives from 2-chloro- 6-ethoxy-4-acetylpyridine. Monatsh. Chem. 139, 1409–1415.
Arya, K., Kumar, S., Arya, A.K., Kumar, M., 2018. Ionic Liquid [PyN$(CH_2)_4SO_3H$][CH_3PhSO_3] Mediated & Promoted Eco-Friendly One-Pot Domino Synthesis of Benzothiazolopyrano/ Chromenopyrimidine Derivatives. Curr. Organocatal. 5, 222–228.
Asgari, G., Seidmohammadi, A., Esrafili, A., Faradmal, J., Noori Sepehr, M., Jafarinia, M., 2020. The catalytic ozonation of diazinon using nano-MgO@CNT@Gr as a new heterogenous catalyst: the optimization of effective factors by response surface methodology. RSC Adv. 10, 7718–7731.
Bhaskaruni, S.V.H.S., Maddila, S., Gangu, K.K., Jonnalagadda, S.B., 2020. A review on multi-component green synthesis of N-containing heterocycles using mixed oxides as heterogeneous catalysts. Arab. J. Chem. 13, 1142–1178.
Cumming, J.G., Mckenzie, C.L., Bowden, S.G., Campbell, D., Masters, D.J., Breed, J., Jewsbury, P.J., 2004. Novel, potent and selective anilinoquinazoline and anilinopyrimidine inhibitors of p38 MAP kinase. Bioorg. Med. Chem. Lett. 14, 5389–5394.
Devineni, S.R., Madduri, T.R., Chamarthi, N.R., Liu, C.-Q., Pavuluri, C.M., 2019. An efficient microwave-promoted three-component synthesis of thiazolo[3,2-a]pyrimidines catalyzed by SiO_2–ZnBr 2 and antimicrobial activity evaluation. Chem. Heterocycl. Com. 55, 266–274.
Ewais, E.M.M., El-Amir, A.A.M., Besisa, D.H.A., Esmat, M., El-Anadouli, B.E.H., 2017. Synthesis of nanocrystalline MgO/$MgAl_2O_4$ spinel powders from industrial wastes. J. Alloy Compd. 691, 822–833.
Feng, Y., Yin, J., Liu, S., Wang, Y., Li, B., Jiao, T., 2020. Facile Synthesis of Ag/Pd Nanoparticle-Loaded Poly(ethylene imine) Composite Hydrogels with Highly Efficient Catalytic Reduction of 4-Nitrophenol. ACS Omega 5, 3725–3733.
Fang, Y., Chi, X., Li, L., Yang, J., Liu, S., Lu, X., Xiao, W., Wang, L., Luo, Z., Yang, W., Hu, S., Xiong, J., Hoang, S., Deng, H., Liu, F., Zhang, L., Gao, P., Ding, J., Guo, Y., 2020. Elucidating the Nature of the Cu(I) Active Site in CuO/TiO_2 for Excellent Low-Temperature CO Oxidation. ACS Appl. Mater. Interfaces 12, 7091–7101.
Harikrishna, S., Robert, A.R., Ganja, H., Maddila, S., Jonnalagadda, S.B., 2020. A green, facile and recyclable Mn_3O_4/MWCNT nanocatalyst for the synthesis of quinolines via one-pot multicomponent reactions. Sustain. Chem. Pharm. 16, 100265.
Hillary, B., Sudarsanam, P., Amin, M.H., Bhargava, S.K., 2017. Nanoscale Cobalt-Manganese Oxide Catalyst Supported on Shape-Controlled Cerium Oxide: Effect of Nanointerface Configuration on Structural, Redox, and Catalytic Properties. Langmuir 33, 1743–1750.
Jannati, S., Esmaeili, A.A., 2018. Synthesis of novel spiro[benzo[4,5]thiazolo[3,2-a]chromeno[2,3-d]pyrimidine-14,3′-indoline]-1,2′,13(2H)-triones *via* three component reaction. Tetrahedron 74, 2967–2972.
Khalaj, M., Sadeghpour, M., Safavi, S.M.M., Lalegani, A., Khatami, S.M., 2019. Copper-catalyzed synthesis of thiazolidine derivatives via multicomponent reaction of terminal alkynes, elemental sulfur, and aziridines. Monatsh. Chem. 150 (6), 1085–1091.
Khalaj, M., Farahani, N., Sadeghpour, M., Tazikeh-Lemeski, E., Khatami, S.M., 2018a. PEG/ZnBr 2-Assisted Multicomponent Reactions: A Novel Procedure for the Synthesis of Functionalized 5,6-Dihydropyran-2-ones. Synlett 29 (07), 894–897.
Khalaj, M., Taherkhani, M., Naderi, F., MousaviSafavi, S.M., 2018b. Catalytic multicomponent reaction between nitroalkanes, elemental sulfur, and oxiranes: Monatsh. Chem. 149 (01), 63–71.
Khandelwal, S., Rajawat, A., Tailor, Y.K., Kumar, M., 2015. Diversity Oriented *p*-TSA Catalyzed Efficient and Environmentally Benign Synthetic Protocol for the Synthesis of Structurally Diverse Heteroannulated Benzothiazolopyrimidines. Curr. Organocatal. 2, 37–43.
Mohamed, S.F., Flefel, E.M., El-Galil, E., Amra, A., Abd El-Shafy, D.N., 2010. Anti-HSV-1 activity and mechanism of action of some new synthesized substituted pyrimidine, thiopyrimidine and thiazolopyrimidine derivatives. Eur. J. Med. Chem. 45, 1494–1501.
Mohire, P.P., Chandam, D.R., Patil, R.B., Patravale, A.A., Ghosh, J. S., Deshmukh, M.B., 2019. Low melting mixture glycerol: proline as an innovative designer solvent for the synthesis of novel chromeno fused thiazolopyrimidinone derivatives: An excellent correlation with green chemistry metrics. J. Mol. Liq. 283, 69–80.
Rai, U.S., Isloor, A.M., Shetty, P., Vijesh, A.M., Prabhu, N., Isloor, S., Thiageeswaran, M., Fun, H.-K., 2010. Novel chromeno[2,3-b]-pyrimidine derivatives as potential anti-microbial agents. Eur. J. Med. Chem. 45, 2695–2699.
Roudbaraki, S.J., Ziyaadini, M., Ghashang, M., 2019. Multi-component Preparation of Pyrazolo[3,4-d]thiazolo[3,2-a]pyrimidines Using Solvent-free and HSBM Techniques. Lett. Org. Chem. https://doi.org/10.2174/1570178616666190319155522.
Rahmani Vahid, B., Haghighi, M., 2016. Urea-nitrate combustion synthesis of MgO/$MgAl_2O_4$ nanocatalyst used in biodiesel production from sunflower oil: Influence of fuel ratio on catalytic properties and performance. Energ. Convers. Manage. 126, 362–372.
Sagar Reddy, A.V., Jeong, Y.T., 2016. Highly efficient and facile synthesis of densely functionalized thiazolo[3,2-a]chromeno[4,3-d]pyrimidin-6(7H)-ones using [Bmim]BF_4 as a reusable catalyst under solvent-free conditions. Tetrahedron 72, 116–122.
Sahu, P.K., 2016a. Eco-friendly grinding synthesis of double layered nano material and correlation between basicity, calcinations and catalytic activity in green synthesis of novel fused pyrimidines. RSC Adv. 6, 78409–78423.
Sahu, P.K., 2016b. Role of surfactant and micelle promoted mild, green, highly efficient and sustainable approach for construction of novel fused pyrimidines at room temperature in water. RSC Adv. 6, 67651–67661.
Selvam, T.P., Karthik, V., Kumar, P.V., Ashraf Ali, M., 2012. Design, synthesis, antinociceptive, and anti-inflammatory properties of thiazolopyrimidine derivatives. Toxicol. Environ. Chem. 94, 1247–1258.
Shafighi, S., Mohammad Shafiee, M.R., Ghashang, M., 2018. MgO-CeO_2 nanocomposite: efficient catalyst for the preparation of 2-aminothiophenes and thieno[2,3-d]pyrimidin-4(3H)-one derivatives. J. Sulfur Chem. 39, 402–413.
Sharma, N., Ojha, H., Bharadwaj, A., Pal Pathak, D., Sharma, R.K., 2015. Preparation and catalytic applications of nanomaterials: a review. RSC Adv. 5, 53381–53403.
Tripathy, S., Bhattacharya, D., 2013. Rapid synthesis and characterization of mesoporous nanocrystalline $MgAl_2O_4$ via flash pyrolysis route. J. Asian Ceram. Soc. 1, 328–332.
Varmazyar, A., Nozad Goli-Kand, A., Sedaghat, S., Khalaj, M., Arab-Salmanabadi, S., 2019a. Copper Salt Catalyzed Synthesis of Functionalized 2H-Pyranes. J. Heterocyclic Chem. 56, 1850–1856.
Varmazyar, A., Nozad Goli-Kand, A., Sedaghat, S., Khalaj, M., Arab-Salmanabadi, S., 2019b. Domino Ring Opening/Cyclization of Oxiranes for Synthesis of Functionalized 2H-pyran-5-carboxylate. Mol. Divers. https://doi.org/10.1007/s11030-019-09978-9.
Wang, C., Yin, J., Han, S., Jiao, T., Bai, Z., Zhou, J., Zhang, L., Peng, Q., 2019. Preparation of Palladium Nanoparticles Decorated Polyethyleneimine/Polycaprolactone Composite Fibers Constructed by Electrospinning with Highly Efficient and Recyclable Catalytic Performances. Catalysts 9, 559.
Wang, H., Li, G., Fakhri, A., 2020. Fabrication and structural of the Ag_2S-MgO/graphene oxide nanocomposites with high photocatalysis and antimicrobial activities. J. Photoch. Photobio. B 207, 111882.
Youssef, M.M., Amin, M.A., 2012. Microwave Assisted Synthesis of Some New Thiazolopyrimidine, Thiazolodipyrimidine and Thia-

zolopyrimidothiazolopyrimidine Derivatives with Potential Antioxidant and Antimicrobial Activity. Molecules 17, 9652–9667.

Zhan, F., Yin, J., Zhang, A., Zhou, J., Wang, M., Jiao, T., 2020. Controllable morphology and highly efficient catalytic performances of Pd–Cu bimetallic nanomaterials prepared *via* seed-mediated co-reduction synthesis. Appl. Surf. Sci. 146719.

Zhang, H., Jia, X., Liu, Z., Li, Z., 2004. The low temperature preparation of nanocrystalline $MgAl_2O_4$ spinel by citrate sol–gel process. Mater. Lett. 58, 1625–1628.

Zhang, L., Yin, J., Wei, K., Li, B., Jiao, T., Chen, Y., Zhou, J., Peng, Q., 2020. Fabrication of Hierarchical $SrTiO_3$@MoS_2 Heterostructure Nanofibers as Efficient and Low-Cost Electrocatalysts for Hydrogen-Evolution Reactions. Nanotechnology 31, 205604.